Challenge Journal of CONCRETE RESEARCH LETTERS

Research Article

Using the efflorescence mechanism of portland cement to obtain a shiny calcium carbonate surface

Juan Carlos Hernandez Palacios [a], Imelda Olivas Armendariz [a], Juan Francisco Hernandez Paz [a], Pedro Perez Rodriguez [a], Jose Luis Sandoval Granados [b], Hortensia Reyes Blas [a], Lorena Rivera Rios [a], Claudia Alejandra Rodriguez Gonzalez [a,*]

[a] *Department of Physics and Mathematics, Institute of Engineering and Technology, Universidad Autónoma de Ciudad Juarez, 32310 Cd Juárez, Chih., Mexico*
[b] *Department of Architecture, Institute of Arquitecture, Design and Arts, Universidad Autónoma de Ciudad Juarez, 32310 Cd Juárez, Chih., Mexico*

ABSTRACT

This study presents a novel curing strategy to produce a smooth and shiny surface on Portland cement paste by controlling efflorescence. The proposed methodology consists of curing fresh cement paste in contact with a smooth, polystyrene mold, which modifies the boundary conditions at the cement–mold interface by limiting evaporation and promoting local moisture retention during early hydration. Although direct exposure to the atmosphere is restricted, carbon dioxide from the environment can still diffuse through the cement pore network and specimen edges. Under these conditions, calcium ion migration toward the interface is facilitated, leading to the controlled precipitation of a thin, calcium carbonate–rich surface layer. The surface and bulk evolution of the cement paste were investigated after 7, 14, and 28 days of curing using scanning electron microscopy (SEM), energy-dispersive X-ray spectroscopy (EDS), X-ray diffraction (XRD), Fourier transform infrared spectroscopy (FTIR), surface gloss measurements, and compressive strength testing. The analyses reveal the formation of a uniform near-surface region enriched in calcium-containing phases, while the bulk phase assemblage remains dominated by typical hydration products. Quantitative gloss measurements show an increase in surface reflectivity with curing time, reaching approximately 57 ± 1.3 gloss units after 28 days. Compressive strength results indicate that the formation of the shiny surface layer does not adversely affect the mechanical performance of the material. Overall, the results indicate that under the proposed curing conditions, controlled efflorescence could be harnessed as a surface engineering approach to obtain visually uniform and chemically stable surfaces without the use of additives or post-processing treatments.

ARTICLE INFO

Article history:
Received – September 4, 2025
Revision requested – October 1, 2025
Revision received – January 1, 2026
Accepted – January 9, 2026

Keywords:
Efflorescence
Portland cement
Controlled carbonation
Calcium carbonate surface layer

Citation: Hernandez Palacios JC, Olivas Armendariz I, Hernandez Paz JF, Perez Rodriguez P, Sandoval Granados JL, Reyes Blas H, Rivera Rios L, Rodriguez Gonzalez CA (2026). Using the efflorescence mechanism of portland cement to obtain a shiny calcium carbonate surface. *Challenge Journal of Concrete Research Letters*, 17(1), 30–40.

1. Introduction

Cement, primarily in the form of Portland cement, remains the most widely used hydraulic binder in modern construction, with global production exceeding 4.2 billion tons annually (Scrivener et al. 2018). Its widespread use is due to its favorable combination of mechanical strength, cost-effectiveness, and versatility across structural and architectural applications. As the key component in concrete, mortars, grouts, and surface finishes, it plays a central role in infrastructure development worldwide. However, the aesthetic and surface

* *Corresponding author*. E-mail address: claudia.rodriguez@uacj.mx (C. A. Rodriguez Gonzalez)
ISSN: 2548-0928 / DOI: https://doi.org/10.20528/cjcrl.2026.01.003

durability of cement-based materials continues to present challenges, particularly in architectural contexts where surface quality and appearance are critical (Neville 2011).

One of the most common surface-related issues in cement-based materials is efflorescence, characterized by the formation of white crystalline deposits—primarily calcium carbonate—on the exposed surface. These deposits, while chemically benign, are perceived as defects due to their high visual contrast and irregular distribution, which compromise the intended aesthetic (Kosmatka et al. 2002; Brocken and Nijland 2004; Brick Industry Association 2006). Efflorescence can also indicate ongoing moisture transport, which may lead to concerns about durability or permeability, even when these concerns are not mechanically substantiated (Al-Jabari 2022).

Efflorescence is primarily driven by the migration of soluble salts, especially calcium hydroxide (portlandite), through capillary pores during early hydration or due to environmental moisture exposure. Once at the surface, these salts react with atmospheric CO_2, precipitating as calcium carbonate ($CaCO_3$) in a process often referred to as carbonation-induced efflorescence (Ramachandran 1996; Taylor 1997). In complex environmental or cement systems, other phases such as alkali sulfates, thenardite (Na_2SO_4), glaserite ($K_3Na(SO_4)_2$), syngenite ($K_2Ca(SO_4)_2{\cdot}H_2O$), and even ettringite may also appear (Ma and Qian 2018; Bai 2009). Efflorescence is generally categorized into two types: primary efflorescence, which occurs during initial hydration and curing, and secondary efflorescence, which emerges due to water ingress after curing, often through rain, condensation, or rising damp (Dahri 2022; Sutan and Sinin 2013).

Efforts to mitigate efflorescence have traditionally focused on reducing water-to-cement ratios, modifying mix design (e.g., with pozzolanic additions or blended cements), controlling curing conditions, or applying surface sealants to reduce permeability (Liang et al. 2022; Zhang et al. 2014, 2018). The use of admixtures such as sodium stearate, or hydrophobic agents has also been explored, though results vary depending on the system and exposure conditions (Xue et al. 2018; Chindaprasirt et al. 2022; Lothenbach et al. 2011). However, most of these methods seek to suppress the efflorescence mechanism rather than leverage it.

This study investigates an alternative curing approach in which efflorescence is deliberately controlled to promote the formation of a smooth, carbonate-rich surface layer. Instead of eliminating the migration of calcium salts, we control it to produce a smooth, shiny, and durable surface finish. By curing the cementitious material in contact with a smooth, non-porous polymeric mold under controlled humidity, we guide the migration and crystallization of calcium carbonate into a thin, homogeneous surface layer. The result is a naturally shiny and aesthetically appealing finish that exploits the same physicochemical mechanisms responsible for undesired efflorescence, transforming them into a design opportunity.

This methodology, currently under patent application (Mx/a/2016/002861), enables the controlled formation of functional calcium carbonate coatings during early hydration. These coatings exhibit uniform shine, enhanced surface texture, and potentially improved durability against weathering or abrasion. Moreover, the process is compatible with conventional cementitious materials and does not require post-processing treatments or additives. The aim of this work is to investigate the microstructural and surface implications of this approach and evaluate its potential for sustainable, low-cost, and architecturally expressive cement-based surfaces.

2. Experimental Procedure and Materials

2.1. Materials

The materials used for the procedure were sourced locally. The Portland cement used was a standard Type I cement commonly distributed in the region. The water used in the experiments was supplied by the city's water and sanitation company.

2.2. Experimental procedure

Samples were prepared using Type I Portland cement and water at a water-to-cement ratio (w/c) of 0.50 by mass. The cement powder was sifted using a sieve to ensure uniform particle size and then mixed with water. The mixture was stirred continuously until a homogeneous composition was achieved. The prepared mixture was poured into polystyrene containers with dimensions of 7 cm in height, 8 cm in width, and 18.5 cm in length. After casting, the specimens remained in the polystyrene molds and were cured under uncontrolled ambient indoor conditions typical of the laboratory environment in Ciudad Juárez (Chihuahua, Mexico). During the curing period, the indoor temperature averaged 23 ± 2 °C, with a relative humidity of 25–35 %, consistent with the local semi-arid climate. The indoor CO_2 concentration was not actively regulated but generally remained within 420–650 ppm, which corresponds to typical atmospheric levels for indoor environments in the region. No external load or confinement was applied; the only contact pressure exerted on the samples was due to their own self-weight against the smooth polystyrene surface. The specimens were cured for 7, 14, and 28 days under these conditions.

Surface gloss was quantitatively evaluated using a portable glossmeter Landtek GM60 (measurement geometry: 60°, in accordance with ISO 2813). Gloss measurements were performed directly on the cement surfaces after 7, 14, and 28 days of curing. For each curing age, measurements were taken at three different locations on the sample surface, and the average value was reported in gloss units (GU), together with the corresponding standard deviation. For the chemical stability test, shiny-surface specimens cured for 28 days were immersed in aqueous solutions with pH 4, 7, and 11 for 5 minutes at room temperature. After immersion, the samples were rinsed with deionized water to remove residual solution and then allowed to air-dry for 6 hours under laboratory conditions until the surface was completely dry. Surface gloss was measured before immersion and after drying using the same measurement con-

ditions described above. The variation in gloss values was used as an indicator of the short-term chemical stability of the surface layer.

The morphology and elemental chemical composition of the samples were analyzed using scanning electron microscopy (SEM, Hitachi model SU5000) and Energy Dispersive X-Ray Spectroscopy (EDS, Bruker), with an acceleration voltage of 15 kV. Phase identification and structural analysis were performed by X-ray diffraction (XRD) using a PANalytical X'Pert Pro diffractometer with Cu Kα radiation (λ = 0.1542 nm). Measurements were carried out on intact cement paste specimens, with the exposed surface facing the incident X-ray beam. As a result, the diffraction patterns mainly reflect the bulk phase composition of the material, while allowing qualitative comparison between samples. Functional groups present in the samples were identified using Fourier Transform Infrared Spectroscopy (FT-IR, Nicolet 6700) in the range of 500-3000 cm^{-1}. FTIR and XRD measurements were performed on replicate specimens for each curing age and condition, showing consistent spectral features; therefore, representative spectra are reported.

3. Results and Discussion

Fig. 1 presents the surface appearance of Portland cement samples cured for 7, 14, and 28 days, together with the corresponding quantitative gloss measurements. After 28 days, the surface exhibits a distinctly smooth and reflective appearance. This visual evolution is corroborated by the gloss measurements, which show a systematic increase in gloss units with curing time. The average surface gloss increased progressively from 22 ± 3 GU at 7 days to 35 ± 1.7 GU at 14 days, reaching 57 ± 1.3 GU at 28 days. The progressive reduction in standard deviation suggests enhanced surface uniformity and a more homogeneous development of the shiny surface layer over time.

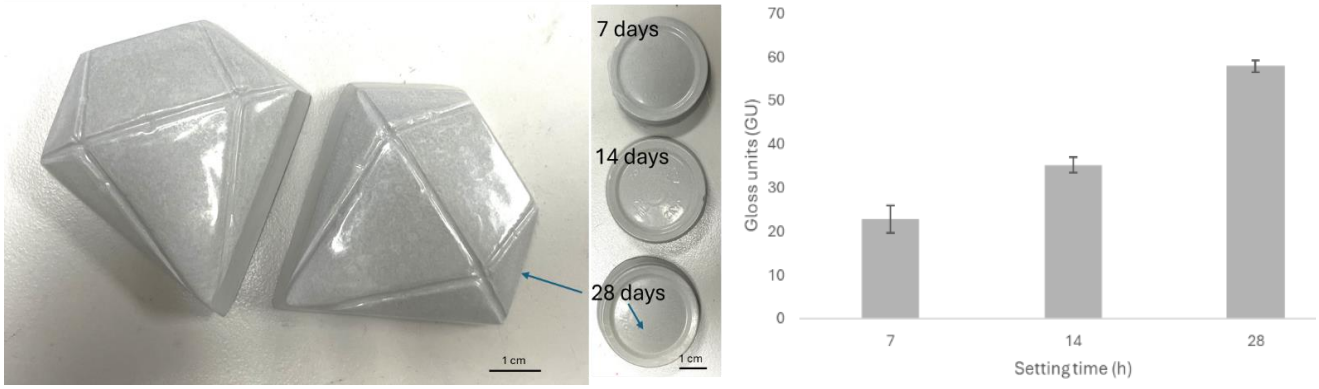

Fig. 1. Progressive development of shiny surfaces in Portland cement samples over 7, 14, and 28 days of curing.

Figs. 2–4 present a comparison between samples set using a conventional process and those treated according to the methodology proposed in this study, utilizing a surface in contact with polystyrene, after 7, 14, and 28 days of curing. From day 7 onward, a significant difference is observed in both the roughness and morphology of the surface, as well as in the phases present, evidenced by the varying gray tones in the backscattered electron images. The conventionally cured sample exhibits a more irregular surface morphology, with predominantly spherical particles and some polyhedral features. This is consistent with the findings reported previously for Portland cement, where the morphology of cement particles is typically characterized by spherical and irregular shapes due to the grinding and clinker formation processes (Taylor 1997; Bogue 1955). In contrast, the surface set using the proposed methodology appears visually smoother and is composed of two main phases: one with an acicular shape (lighter gray) and the other with spherical particles.

After 14 days, the roughness on both surfaces has decreased. The surface set conventionally exhibits microcracks or irregularities and is primarily composed of spherical particles with the presence of some needle-like structures. This aligns with findings reported in the literature, where the morphology of conventional Portland cement over time typically shows a decrease in surface roughness and the formation of microcracks as hydration progresses (Taylor 1997; Bogue 1955; Lura et al. 2003). In contrast, the surface set using the procedure proposed in this study still shows two distinct phases: spherical particles and acicular ones. However, the acicular phase appears to have undergone some growth, and the needle-like structures are now less noticeable.

After 28 days of conventional curing, at low magnifications, the surface appears to have minimal roughness. At higher magnifications, larger particles are observed, covered by small spherical particles, with the presence of some needle-like structures. This aligns with previous studies, where the morphology of Portland cement at later stages of hydration typically shows the development of larger particles covered by finer spherical ones, along with the formation of needle-like structures such as ettringite (Taylor 1997). In contrast, for the curing process proposed in this study, the surface roughness has decreased even at higher magnifications. Both phases, spherical particles and acicular structures, are still present, but the needle-like structures have grown and now cover almost the entire surface. This is consistent with the evolution of the microstructure described in the literature, where needle-like crystals tend to grow and eventually dominate the surface as hydration progresses (Bogue 1955; Lura et al. 2003).

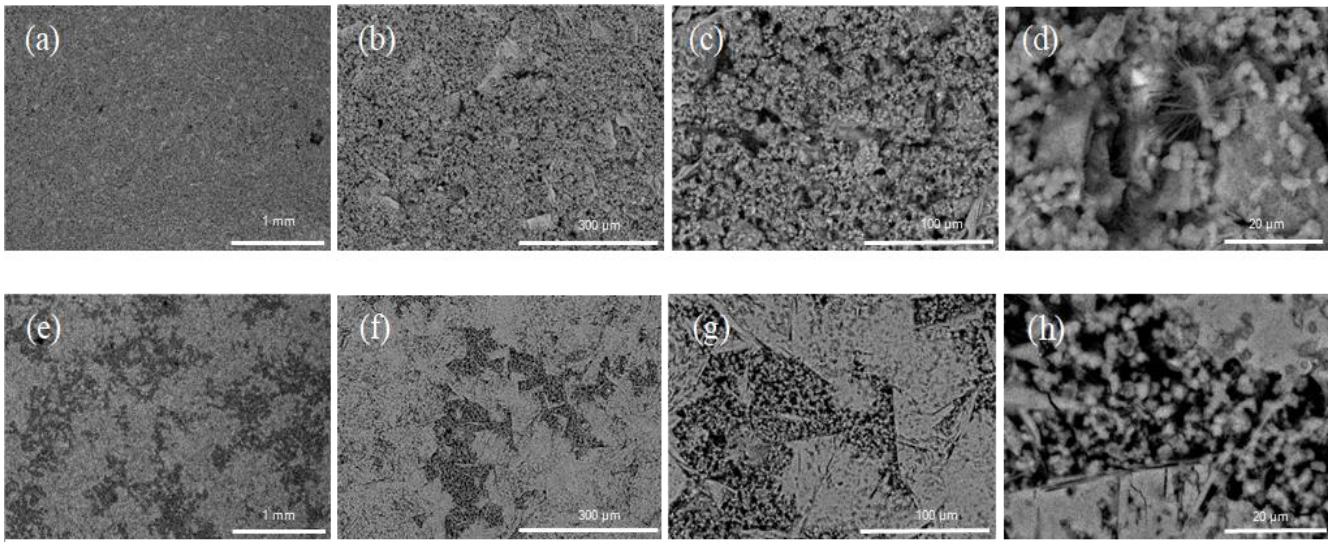

Fig. 2. SEM–BSE surface morphology after 7 days of curing for conventional (a–d) and shiny (e–h) cement paste samples. Imaging conditions: 20 kV, WD 19–23 mm, 30 Pa.

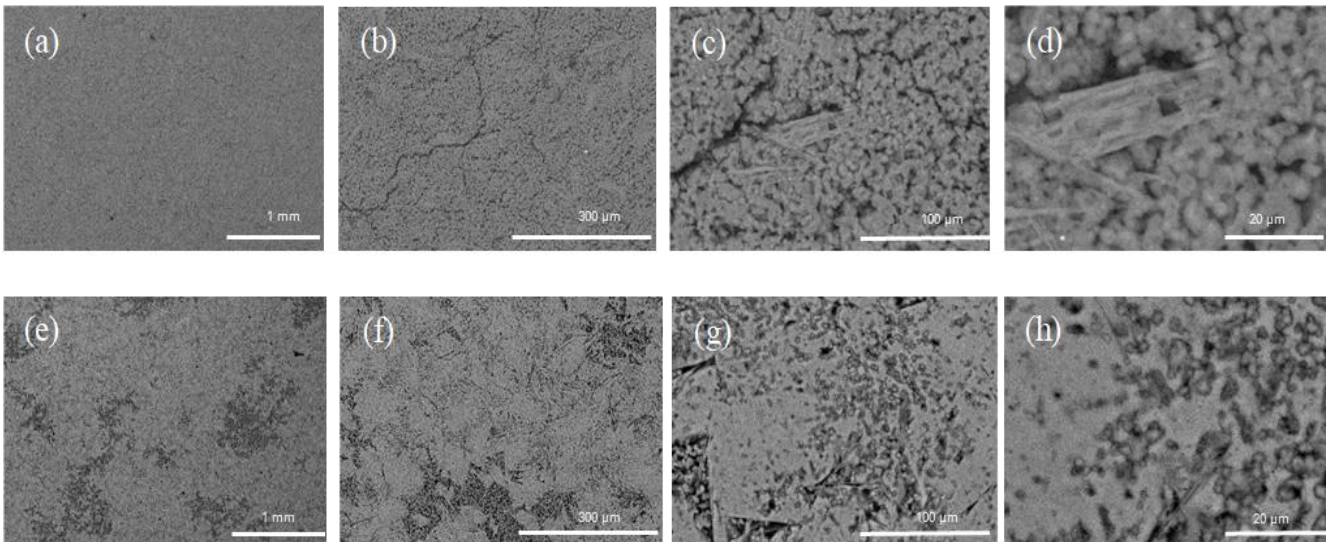

Fig. 3. SEM–BSE surface morphology after 14 days of curing for conventional (a–d) and shiny (e–h) cement paste samples. Imaging conditions: 20 kV, WD 19–23 mm, 30 Pa.

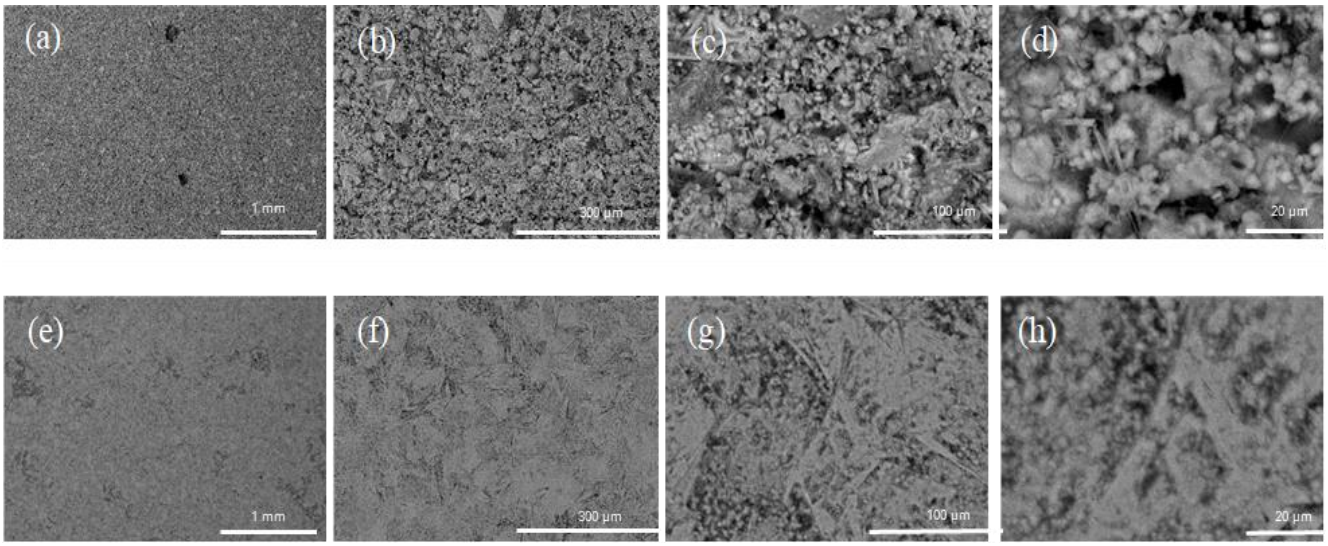

Fig. 4. SEM–BSE surface morphology after 28 days of curing for conventional (a–d) and shiny (e–h) cement paste samples. Imaging conditions: 20 kV, WD 19–23 mm, 30 Pa.

Fig. 5 presents the XRD patterns of Portland cement paste specimens cured for 7, 14, and 28 days, together with a conventional reference sample. All diffractograms are dominated by a broad amorphous background attributed to calcium silicate hydrate (C–S–H), along with crystalline reflections corresponding to portlandite ($Ca(OH)_2$) and calcium carbonate ($CaCO_3$) (Taylor, 1997). Weak and partially overlapped reflections associated with residual clinker phases, mainly tricalcium silicate (C_3S) and dicalcium silicate (C_2S), are also detected.

The conventional sample exhibits more clearly defined reflections associated with residual clinker phases compared to the specimens cured against the smooth polymeric surface. Given the limited surface sensitivity of conventional powder XRD, these differences should be interpreted with caution and primarily reflect variations in the bulk phase contribution. With increasing curing time, the relative intensity of $CaCO_3$ reflections increases for all samples, while the overall phase assemblage remains unchanged (Lura et al. 2003).

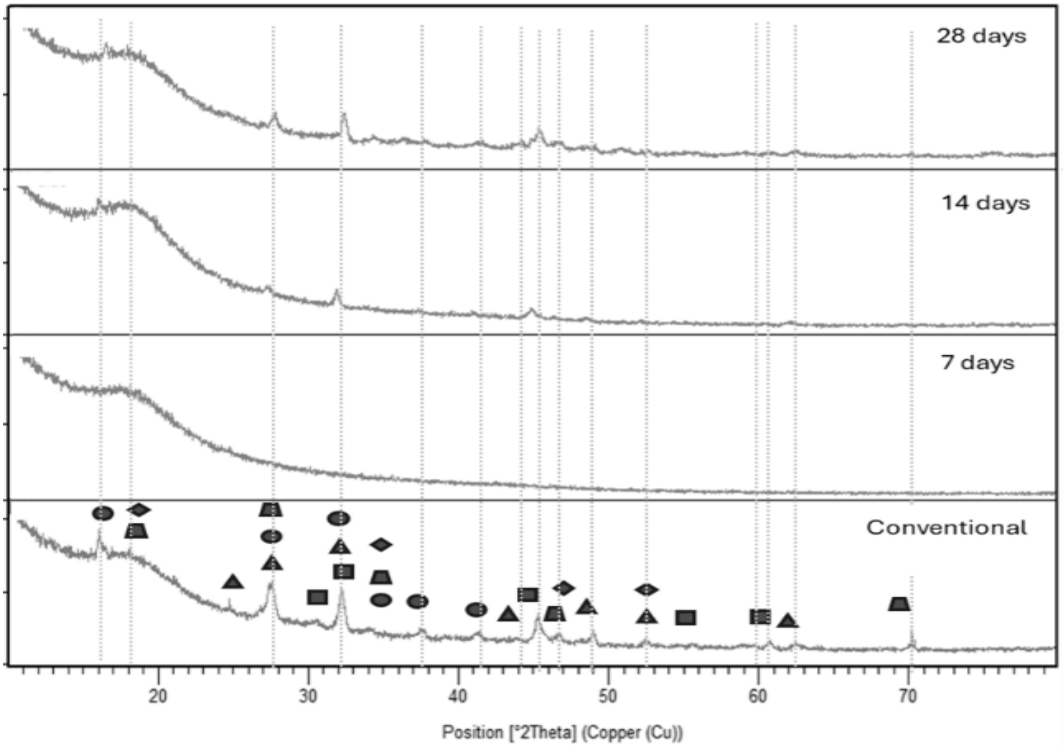

	Phase	Chemical formula	PDF reference	Main 2θ (°)	d-spacing (Å)	Conventional	7 days	14 days	28 days
▲	**Portlandite**	$Ca(OH)_2$	00-044-1481	~18.0	4.90	✓	✓	✓	✓
				~34.1	2.63	✓	✓	✓	✓
				~47.1	1.93	~	~	~	~
▲	**Calcium carbonate ($CaCO_3$)**	$CaCO_3$	00-033-0268	~29.4	3.03	✓	✓	✓	✓
				~39.4	2.28	~	~	✓	✓
				~43.1	2.10	~	~	~	✓
◆	**Alite**	Ca_3SiO_5	00-031-0301	~29.3	3.05	~	~	~	~
				~32.1	2.78	~	~	~	~
				~51.7	1.77	—	—	—	~
■	**Belite**	Ca_2SiO_4	01-087-1260	~32.3	2.77	~	~	~	~
				~41.1	2.19	—	—	~	~
				~51.5	1.77	—	—	—	~
●	**Ettringite (minor)**	$Ca_6Al_2(SO_4)_3(OH)_{12}\cdot 26H_2O$	00-041-1451	~15.8	5.60	~	~	~	~
				~22.9	3.88	—	—	—	—
				~31.1	2.87	—	—	~	~

Notation: ✓ = clearly observed, ~ = weak/overlapped, — = not resolved

Fig. 5. XRD patterns of Portland cement paste under modified curing conditions after 7, 14, and 28 days.

The FTIR spectra (Fig. 6) of both conventional and shiny samples consistently display the main hydration and carbonation bands characteristic of Portland cement systems. In all cases, the sharp O–H stretching vibration of portlandite is observed at 3643 cm^{-1}, together with a broad O–H band above 3000 cm^{-1} and the H_2O bending mode around 1650 cm^{-1}. The Si–O stretching of C–S–H is identified near 970–990 cm^{-1}, while sulfate vibrations appear in the region of 1110–1140 cm^{-1}. Carbonate formation is indicated by the bands at 1450 cm^{-1} (ν_3, asymmetric stretching), 1070–1090 cm^{-1} (ν_1, symmetric stretching), and 874–878 cm^{-1} (ν_2, out-of-plane bending) (Ylmen and Jäglid 2013; Chakrabarty and Mahapatra 1999; Jennings 2000). These features are present in both curing conditions and at all curing ages (7, 14, and 28 days), with variations in relative intensity and definition that reflect progressive hydration and carbonation processes. In addition, an FTIR spectrum of the mold material was recorded to document the polymer used for sample casting (Fig. 7). The spectrum shows the characteristic absorption bands of polystyrene, confirming the nature of the mold material employed in this study.

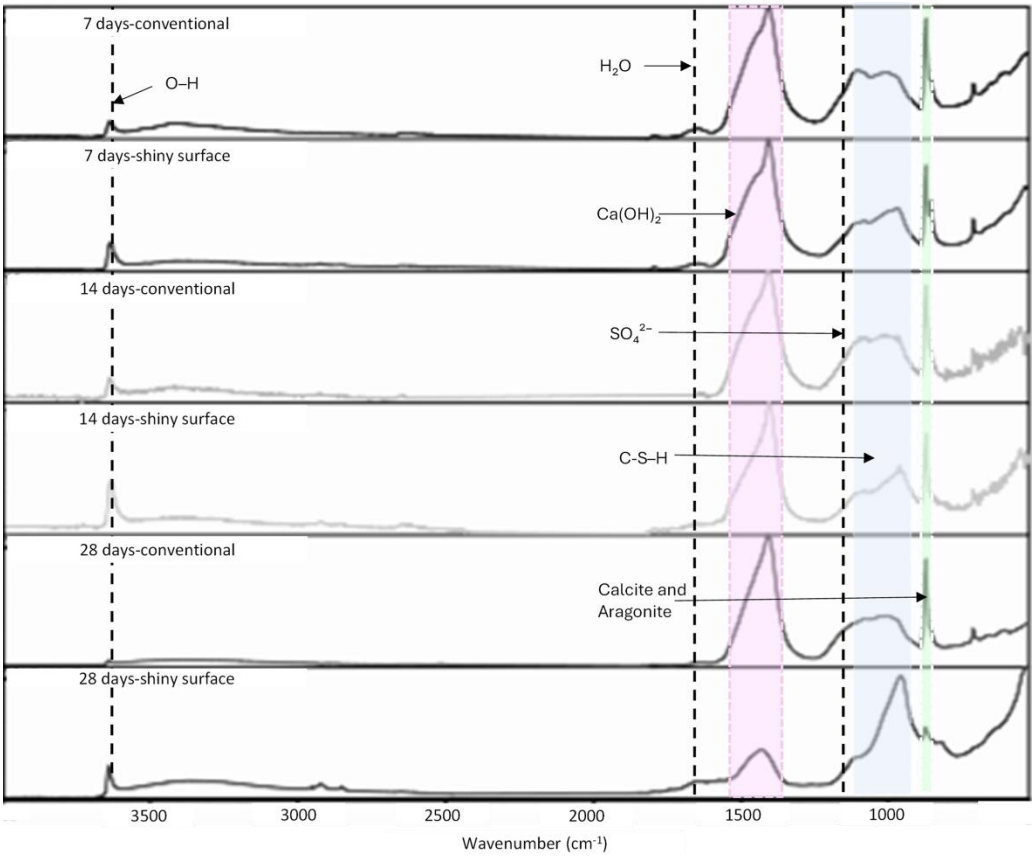

Fig. 6. FTIR analysis of the shiny surface and the Portland cement samples.

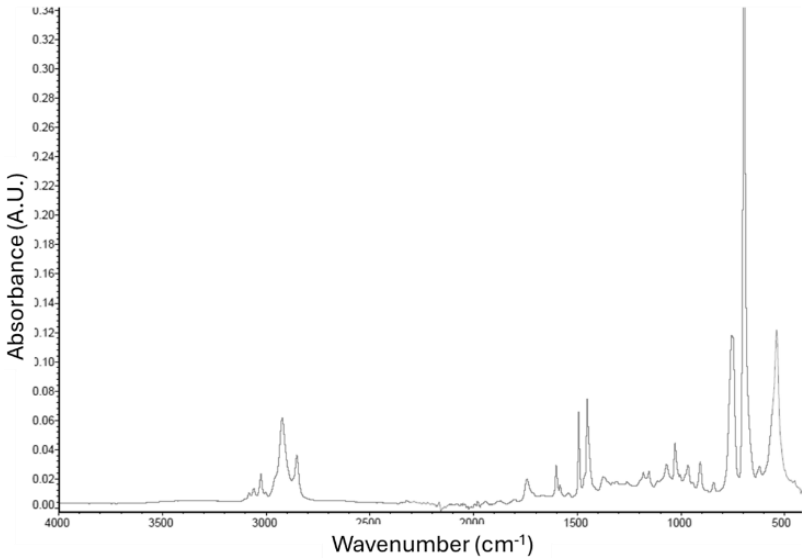

Wavenumber (cm^{-1})	Functional group / vibration	Assignment
3000–3100	Aromatic C–H stretching	Vibrations associated with the benzene ring of polystyrene
2924, 2846	Aliphatic C–H stretching (–CH_2–)	Asymmetric and symmetric stretching of methylene groups in the polymer backbone
1600, 1490, 1447	Aromatic C=C ring stretching	Characteristic phenyl ring vibrations of polystyrene
1000–1030	Aromatic ring deformation / C–H in-plane bending	Phenyl ring deformation modes
750, 700	Aromatic C–H out-of-plane bending	Diagnostic bands of mono-substituted benzene rings (pendant phenyl groups)

Fig. 7. FTIR spectrum of the polystyrene mold used for casting the Portland cement samples.

Fig. 8 presents cross-sectional SEM images and corresponding EDS spectra of Portland cement samples cured using the proposed methodology, which results in a visibly shiny surface layer. The SEM micrographs reveal a compact and dense outer region, particularly within the top ~50 μm of the surface, where the structure appears homogeneously packed. This dense morphology is attributed to minimized evaporation and restricted ion migration, induced using a smooth, non-porous polymeric mold during the early stages of hydration (Khayat 1999).

Within the microstructure, hydration products such as calcium silicate hydrate (C–S–H) and portlandite are clearly observed. The coexistence of fibrous, amorphous, and acicular phases suggests a well-developed and active hydration process, with no significant signs of microcracking, shrinkage, or surface deterioration. These features indicate that the curing method not only preserves structural integrity but may also promote surface densification, consistent with observations in high-performance and self-consolidating concretes where controlled curing conditions influence near-surface compactness.

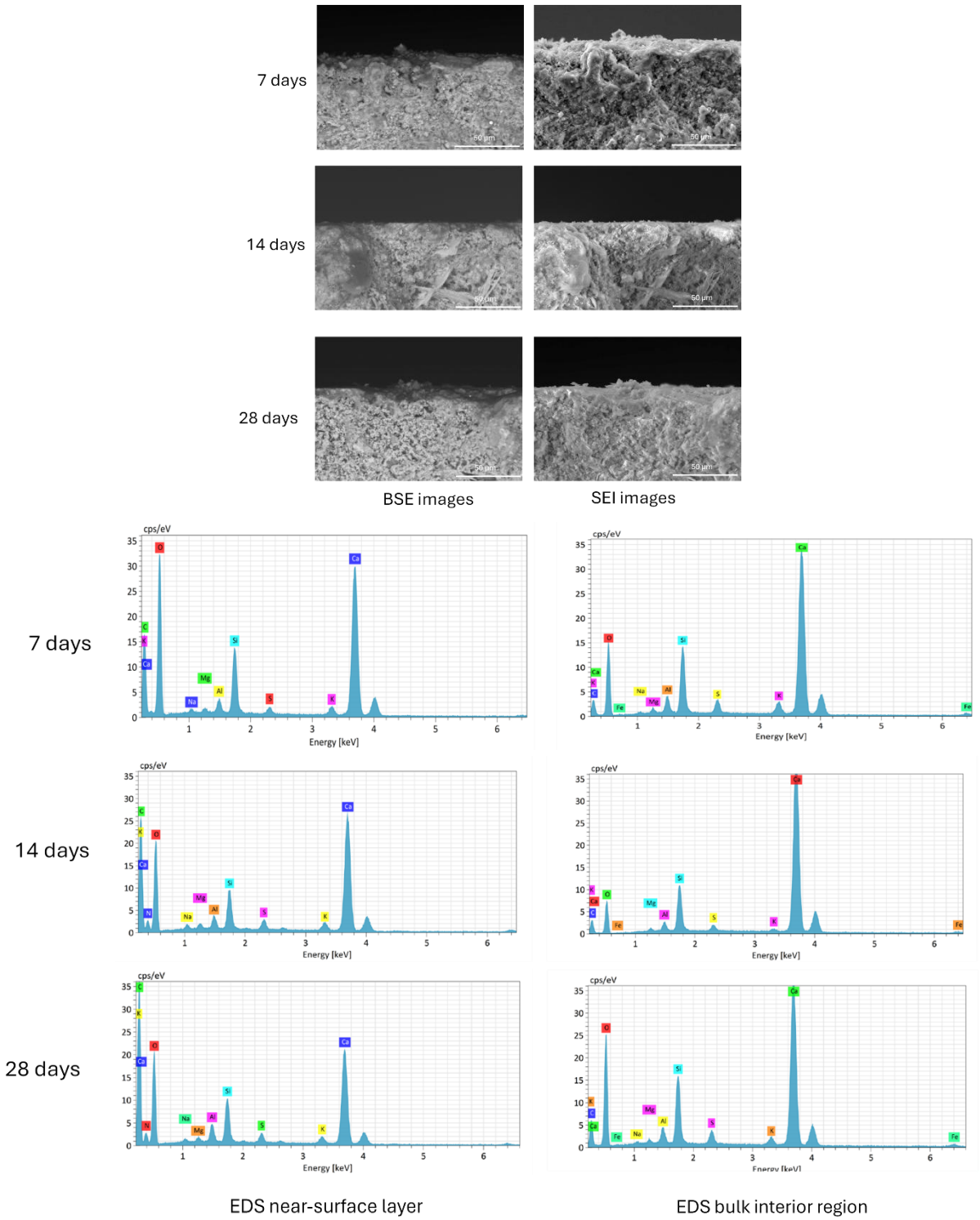

Fig. 8. Cross-sectional SEM images and corresponding EDS analyses of Portland cement paste cured using the proposed methodology after (a) 7, (b) 14, and (c) 28 days. Imaging conditions: 20 kV, working distance 11–14.2 mm, 30 Pa.

EDS elemental mapping (Fig. 9) confirms a marked increase and surface-level enrichment of calcium, particularly in specimens cured against smooth polymeric molds. This calcium-rich layer supports the formation of a dense, carbonate-containing coating, which is consistent with the enhanced reflectivity and "shiny" appearance observed macroscopically. This correlates with FTIR results, where stronger absorption bands for CO_3^{2-} groups are observed. While early stage XRD data revealed low surface crystallinity, the FTIR and SEM/EDS analyses demonstrate that carbonate formation is already underway at both the microstructural and molecular levels, though initially in amorphous or nano-crystalline form. The observed surface densification and spatial continuity in SEM images support the interpretation that smooth-surface curing promotes a controlled and delayed crystallization, which preserves surface integrity and contributes to long-term uniformity. In contrast, the conventionally cured control sample shows a less uniform calcium distribution and a more porous, irregular surface structure. This finding is consistent with the sharper diffraction peaks and earlier crystallization observed via XRD. The microstructural differences reinforce that the proposed curing strategy not only modulates hydration kinetics and carbonation pathways, but also improves aesthetic, protective, and potentially functional properties of the cement surface by forming a shiny, compact mineral layer.

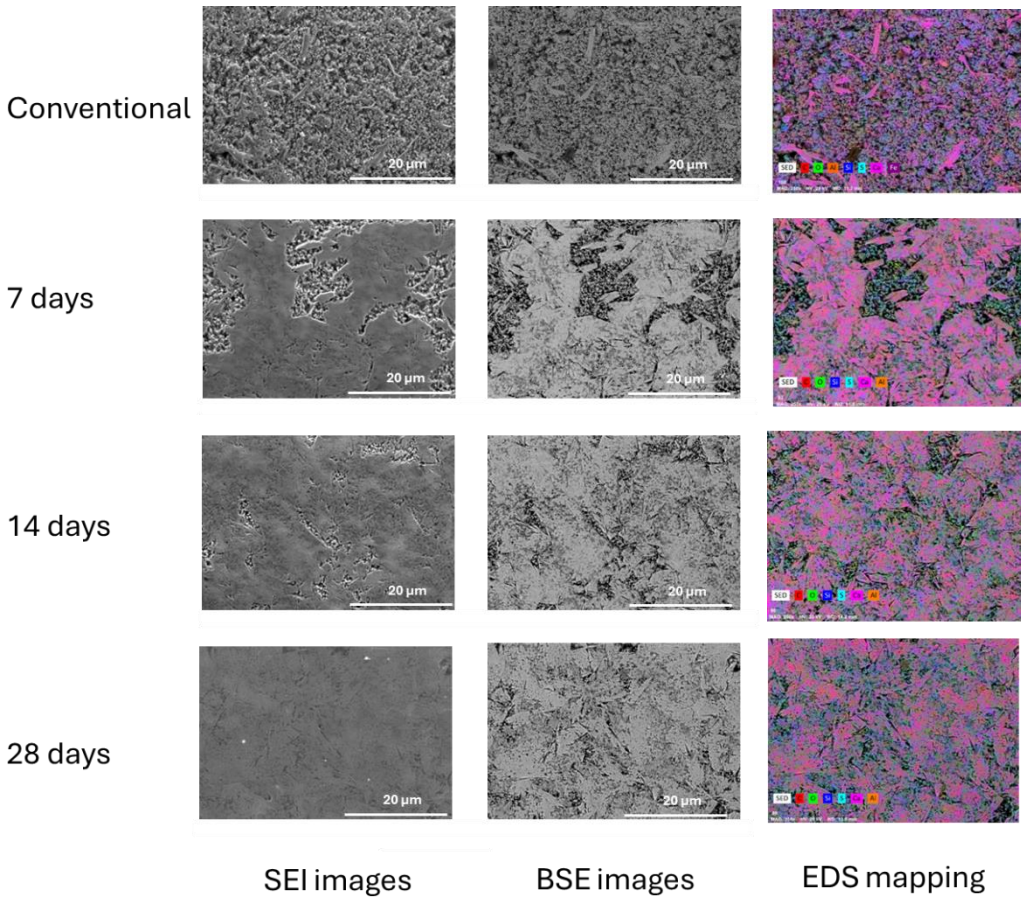

Fig. 9. SEM images and EDS elemental maps comparing a conventional Portland cement sample cured for 28 days with samples prepared using the proposed methodology after 7, 14, and 28 days of curing. Imaging conditions: 20 kV, working distance 10.8–14.2 mm, 30 Pa.

The formation of the shiny surface can be attributed to modified curing boundary conditions imposed by the smooth polymeric mold, which reduce surface evaporation and promote higher local moisture retention. Although direct exposure to the atmosphere is limited, CO_2 can still diffuse through the cement pore network and from specimen edges, enabling localized carbonation. These conditions are consistent with enhanced migration and accumulation of calcium-rich species near the surface, leading to the formation of a thin, dense carbonate-containing layer. This proposed mechanism (Fig. 10) is supported by SEM–EDS evidence of near-surface Ca enrichment, FTIR carbonate bands, and increased surface gloss with curing time. Due to the bulk sensitivity of conventional XRD, these effects are interpreted as near-surface phenomena rather than bulk phase transformations.

Table 1 summarizes the maximum compressive strength obtained for the analyzed samples. At 7 and 14 days, specimens with a shiny surface exhibited slightly higher compressive strength values than the conventional samples, with increases of approximately 0.9 % and 1.3 %, respectively. However, these differences fall within the range of experimental variability typically reported for compressive strength tests on Portland cement pastes and mortars (Mindess et al. 2003; Neville

2011). At 28 days, both sample types reached very similar maximum compressive strength values, indicating that the surface condition does not exert a significant influence on long-term mechanical performance. Overall, these results suggest that the formation of the shiny layer induced by controlled efflorescence is confined to the near-surface region and does not adversely affect the bulk mechanical response of the material.

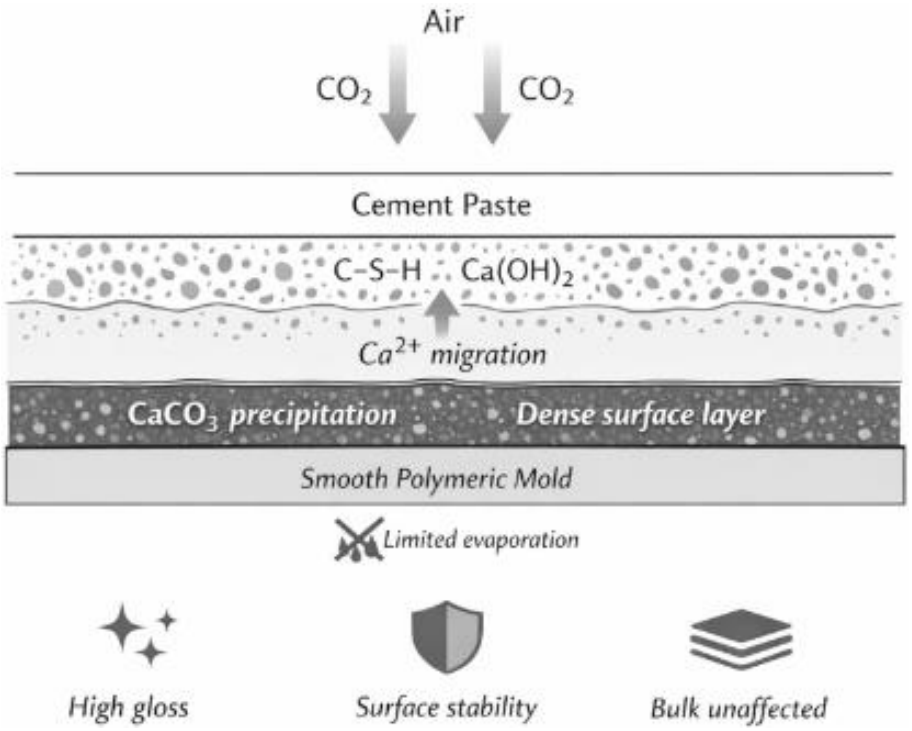

Fig. 10. Schematic illustration of the proposed mechanism for the formation of the shiny surface on Portland cement paste cured against a smooth polymeric mold (AI-assisted).

Table 1. Maximum compressive strength of conventional and shiny samples at different curing ages.

Sample / Curing age	7 days (conventional)	7 days (shiny)	14 days (conventional)	14 days (shiny)	28 days (conventional)	28 days (shiny)
Maximum compressive strength (MPa)	70.4 ± 3.1	71.0 ± 2.8	79.9 ± 2.5	81.0 ± 2.2	89.3 ± 2.0	89.0 ± 1.9

Fig. 11 shows the variation in surface gloss (expressed in gloss units, GU) of the shiny surfaces of Portland cement samples cured for 28 days, measured before and immediately after exposure to aqueous solutions with pH 4, 7, and 11, which were used to evaluate the chemical resistance of the surface layer. The results indicate that the initial gloss value of the shiny surface (≈ 58 GU) remains essentially unchanged after contact with the different media, with only minor fluctuations of less than ±2 GU, which fall within the experimental error margin. This stability indicates that the shiny surface layer exhibits a high resistance to immediate chemical attack, with no evidence of dissolution, loss of reflectance, or visible surface degradation. The preservation of gloss under pH 4 conditions suggests adequate tolerance to acidic environments, while the absence of significant gloss reduction at pH 11 demonstrates stability in alkaline media, consistent with the basic nature of Portland cement and its carbonated surface layer. Overall, these results confirm that the shiny finish not only provides aesthetic stability but also functions as a chemically stable surface barrier under short-term exposure to different chemical environments, preserving its optical properties and visual integrity even under controlled aggressive conditions.

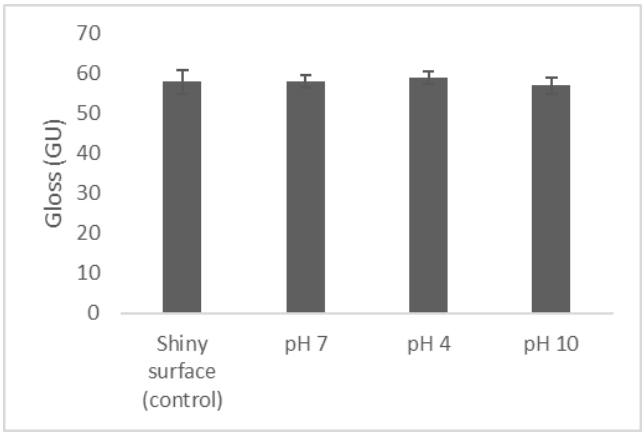

Fig. 11. Surface gloss values (GU) of shiny Portland cement samples cured for 28 days, measured before and after exposure to aqueous solutions with pH 4, 7, and 11.

4. Conclusions

This study presents an approach to reframe efflorescence in Portland cement as a controlled mechanism for achieving a functional and aesthetically appealing surface finish. By employing a smooth polymeric interface during curing, the migration of calcium-rich species and their subsequent reaction with atmospheric carbon dioxide were guided to promote the formation of a homogeneous, shiny surface layer rich in crystalline calcium carbonate. Microstructural and chemical analyses (SEM, EDS, XRD, and FTIR) confirmed the progressive development of this near-surface layer, while the bulk cement matrix retained the typical hydration products such as C–S–H, portlandite, and ettringite.

Importantly, quantitative surface gloss measurements and compressive strength testing demonstrate that the formation of the shiny layer is confined to the outer region of the material and does not adversely affect its mechanical performance. These findings indicate that the observed surface modification is not merely cosmetic, but rather reflects a localized mineralogical evolution driven by altered curing boundary conditions. Within the scope of this study, controlled efflorescence is shown to be a promising surface engineering approach that does not require additives or post-processing treatments. Beyond its potential architectural and prefabrication applications, this strategy provides new insight into the role of moisture transport, ion migration, and carbonation during early cement hydration and may inform future strategies for designing functional cement-based surfaces. From a sustainability perspective, the proposed methodology relies exclusively on controlled curing conditions, which may reduce material consumption, surface rework, and associated environmental impacts.

Acknowledgements

The authors declare that the methodology described in this study is subject to a patent application (Mx/a/2016/002861).

The biocompatibility and bioactivity of a similar material obtained under controlled conditions were reported in Vol. 7, No. 1 (2020) of Memorias del XLII Congreso Nacional de Ingeniería Biomédica, associated with the conference held on October 15-17, 2020.

This research has previously been presented at the XXX International Materials Research Congress (IMRC2022) held in Cancun, QR, Mexico, on August 14-19, 2022. Extended version of the research has been submitted to Challenge Journal of Concrete Research Letters and has been peer-reviewed prior to the publication.

Funding

The authors received no financial support for the research, authorship, and/or publication of this manuscript.

Conflict of Interest

The authors declare no potential conflicts of interest with respect to the research, authorship, and/or publication of this manuscript.

Data Availability

The datasets generated and/or analyzed during the current study are not publicly available but are available from the corresponding author upon reasonable request.

AI Assistance

During the preparation of this manuscript, ChatGPT-5 (OpenAI) was used exclusively for image creation. The authors take full responsibility for the content, interpretation, and conclusions of the published article.

Author Contributions

All authors made substantial contributions to the conception and design of the study, acquisition of data, analysis and interpretation of data; drafted or critically revised the manuscript for important intellectual content; and approved the final version to be published.

References

Al-Jabari M (2022). Concrete durability problems: physicochemical and transport mechanisms. In: *Integral Waterproofing of Concrete Structures*. Springer, Cham, Switzerland, 69–107.

Bai J (2009). Durability of sustainable concrete materials. In: Khatib JM, editor. Sustainability of Construction Materials. Woodhead Publishing, Cambridge, UK, 239–253.

Bogue RH (1955). The Chemistry of Portland Cement. Reinhold Publishing Corporation, New York, USA.

Brick Industry Association (2006). Efflorescence – Causes and prevention. Technical Note 23A. https://www.gobrick.com/docs/default-source/read-research-documents/technicalnotes/tn23a.pdf [accessed 01-09-2024].

Brocken HJP, Nijland TG (2004). White efflorescence on brick masonry and concrete masonry blocks, with special emphasis on sulfate efflorescence on concrete blocks. *Construction and Building Materials*, 18(5), 315–323.

Chakrabarty D, Mahapatra S (1999). Aragonite crystals with unconventional morphologies. *Journal of Materials Chemistry*, 9(11), 2953–2957.

Chindaprasirt P, Jitsangiam P, Rattanasak U (2022). Hydrophobicity and efflorescence of lightweight fly ash geopolymer incorporated with calcium stearate. *Journal of Cleaner Production*, 364, 132449.

Dahri AA (2022). Experimental study of effects of efflorescence control admixture in cement mortar. *Quaid-e-Awam University Research Journal of Engineering Science and Technology*, 20(2), 71–76.

Jennings HM (2000). A model for the microstructure of calcium silicate hydrate in cement paste. *Cement and Concrete Research*, 30(1), 101–116.

Khayat KH (1999). Workability, testing, and performance of self-consolidating concrete. *ACI Materials Journal*, 96(3), 346–353.

Kosmatka SH, Kerkhoff B, Panarese WC (2002). Design and Control of Concrete Mixtures. Portland Cement Association, Skokie, IL, USA.

Liang K, Cui K, Sabri MMS, Huang J (2022). Influence factors in the wide application of alkali-activated materials: A critical review about efflorescence. *Materials*, 15(18), 6436.

Lothenbach B, Scrivener K, Hooton RD (2011). Supplementary cementitious materials. *Cement and Concrete Research*, 41(12), 1244–1256.

Lura P, Jensen OM, Van Breugel K (2003). Autogenous shrinkage in high-performance cement paste: An evaluation of basic mechanisms. *Cement and Concrete Research*, 33(2), 223–232.

Ma Y, Qian J (2018). Influence of alkali sulfates in clinker on the hydration and hardening of Portland cement. *Construction and Building Materials*, 180, 351–363.

Mehta PK, Monteiro PJM (2014). Concrete: Microstructure, Properties, and Materials. 4th ed. McGraw-Hill Education, New York, USA.

Mindess S, Young JF, Darwin D (2003). *Concrete*. 2nd ed. Prentice Hall, Upper Saddle River, NJ, USA.

Neville AM (2011). Properties of Concrete. 5th ed. Pearson Education, London, UK.

Provis JL, van Deventer JSJ (2014). Alkali Activated Materials. Springer, Dordrecht, Netherlands.

Ramachandran VS (1996). Concrete Admixtures Handbook. 2nd ed. William Andrew Publishing, Norwich, NY, USA.

Scrivener KL, John VM, Gartner EM (2018). Eco-efficient cements: Potential, economically viable solutions for a low-CO_2, cement-

based materials industry. *Cement and Concrete Research*, 114, 2–26.

Sutan NM, Sinin H (2013). Efflorescence phenomenon on concrete structures. *Advanced Materials Research*, 626, 747–750.

Taylor HFW (1997). Cement Chemistry. 2nd ed. Thomas Telford, London, UK.

Xue X, Liu YL, Dai JG, Poon CS, Zhang WD, Zhang P (2018). Inhibiting efflorescence formation on fly ash–based geopolymer via silane surface modification. *Cement and Concrete Composites*, 94, 43–52.

Ylmen R, Jäglid U (2013). Carbonation of Portland cement studied by diffuse reflection Fourier transform infrared spectroscopy. *International Journal of Concrete Structures and Materials*, 7(2), 119–125.

Zhang Z, Provis JL, Reid A, Wang H (2014). Fly ash-based geopolymers: The relationship between composition, pore structure and efflorescence. *Cement and Concrete Research*, 64, 30–41.

Zhang Z, Provis JL, Ma X, Reid A, Wang H (2018). Efflorescence and subflorescence induced microstructural and mechanical evolution in fly ash-based geopolymers. *Cement and Concrete Composites*, 92, 165–177.